SUGISAKA MASANORI

Journal of Robotics, Networking and Artificial Life
Vol. 10(3); December (2023), pp. 275–281
ISSN (Online): 2352-6386; ISSN (Print): 2405-9021
https://alife-robotics.org/jrnal.html

Research Article

Kinetic Analysis of Omnidirectional Mobile Robot with Symmetry Roller's Arrangement

Kenji Kimura[1], Kazuo Ishii[2]
[1]Department of Control Engineering, National Institute of Technology, Matsue College,4-4 Nishi-ikuma-cho, Matsue-shi, Shimane, 690-8518, Japan
[2]Graduate School of Life Science and engineering, Kyushu Institute of Technology, 2-4 Hibikino, Wakamatsu-ku, Kitakyushu-shi 808-0196, Fukuoka, Japan

ARTICLE INFO

Article History

Received 10 November 2023
Accepted 18 May 2024

Keywords

Mobile robot
Omni-roller
Translational motion
Motion analysis of mobile robot

ABSTRACT

In recent years, the efficient mobility of omnidirectional mobile robots is desired in the logistics industry. Hence, various types of rollers are installed in mobile robots. These include omnidirectional rollers, which are characterized with excellent omnidirectional mobility and are considered easy to control. Herein, considering that the side surface of the mechanism is circular, the kinematics of the mechanism assuming an arbitrary arrangement on this circle is derived. Previous research has evaluated the roller arrangement from the perspective of the speed efficiency of the drive roller. Meanwhile, this research focuses on a mobile robot equipped with three omni-rollers. Furthermore, focusing only on the translational speed of the robot, its motion efficiency is evaluated. The distribution of the robot's translational speed is studied, the area of the region is used as the evaluation function, and its behaviors are analyzed.

1. Introduction

Recently, industries, such as logistics, have been looking forward to the practicality of using omnidirectional moving mechanisms, and several mobile robots have been developed with this aim. Holonomic mobile robots have attracted attention owing to their ease of control. This is because omnidirectional movement has three degrees of freedom, expressed as the sum of a two-dimensional translational component and a one-dimensional rotational component, which can be controlled independently. Thus, many movement mechanisms (with three omni-rollers) have been developed, and research on its kinematics and control has been conducted [1].

In this research, the RoboCup meddle-size-league soccer robot is characterized with an omnidirectional moving mechanism. The RV-infinity [2], Musashi150 [3], and NuBot [4] use the most basic triangular arrangement (equilateral triangle). Although no theoretical studies have been conducted on roller arrangements, studies on sphere transport [5], [6] and moving mechanisms [7], [8], [9] have been reported in recent times, focusing on the driving rollers.

In moving mechanisms that use spheres as wheels (or mechanisms that use spheres as transport objects), the optimum angle of the sphere rotation axis with respect to movement direction has been determined, assuming an omnidirectional movement [7]. Furthermore, the optimum location for the two rollers driving the sphere is demonstrated to be at the equator [8].

Meanwhile, in the mobile mechanism that uses rollers as wheels, kinematics is represented using a linear transformation matrix, which maps the input (roller velocity) to the output (robot velocity) (translation and rotation components) [9]. Additionally, mechanisms with a line-symmetrical roller arrangement, as shown in Fig. 1(b)(a)(c), are analyzed. In [10], translational and rotational motions are analyzed by adopting the "volume" of the image through first-order transformations and "area of positive projection" as criteria for evaluating the speed efficiency in movement.

In [11], an evaluation function was derived for a three-roller configuration with a line-symmetrical structure and was used to analyze only translational motion. However, the analysis for mechanisms with an origin-symmetrical

Corresponding author E-mail: k-kimura@matsue-ct.jp, ishii@brain.kyutech.ac.jp

roller arrangement, as shown in Fig.1(d)(a)(e), remains unsolved.

In this study, the efficiency of the mobile robot (equipped with three omni-rollers), as shown in Fig. 1(d)(a)(e), is investigated for only the translational movement. For this purpose, an evaluation function is derived for the general arrangement. The distribution of the translational velocity of the robot is also investigated, and the area of the region is used as an evaluation function to analyze the robot's behaviors.

The rest of this study is as follows. Section 2 discusses the kinematics of mobile robots corresponding to transformation mapping. Section 3 derives a more general sectional area function. Section 4 conducts the simulation. Finally, Section 5 presents the summary and future tasks.

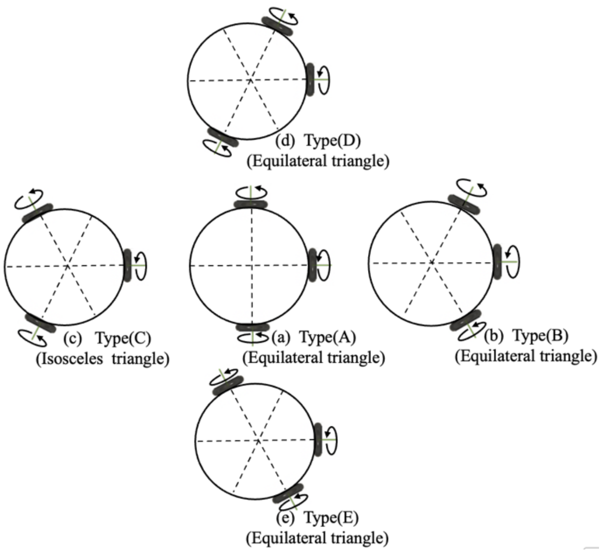

Fig. 1 Mobile robots with three omni-roller arrangement (b)(a)(c), line-symmetry roller arrangement. (d)(e), and point-symmetry roller arrangement.

2. Transformation mapping and kinematics

As shown in Fig. 2(a), the mobile robot with a common radius L adapted the i-th rollers ($i = 1, 2, 3$) at contact point $\boldsymbol{P}_i$, which is positioned as angle θ_i on a global X–Y coordinate system (origin $\boldsymbol{O}$).

Here, the roller peripheral speed $[v_1, v_2, v_3]^{\boldsymbol{T}}$ is given, while the robot translation speed $\boldsymbol{V} = [V_x, V_y]^{\boldsymbol{T}}$ and rational speed $L\dot{\phi}$ ($\dot{\phi}$: robot angular velocity) can be calculated. Thus, $[V_x, V_y, L\dot{\phi}]^{\boldsymbol{T}}$ is determined.

As shown in Fig. 2(b), correspondences of $[v_1, v_2, v_3]$ and $[V_x, V_y, \dot{\phi}L]$ are represented using linear transformation mapping as $f_A : [V_x, V_y, \dot{\phi}L]^{\boldsymbol{T}} \to [v_1, v_2, v_3]^{\boldsymbol{T}}$. $f_{A^{-1}}(W) =$ Image $f_{A^{-1}} \in \mathbf{R}^3$ is a parallelepiped domain from cubic domain W.

Furthermore, the sectional domain of $f_{A^{-1}}(W)$ for horizontal plane $\{V_x V_y - \text{plane}\}$ is as follow.

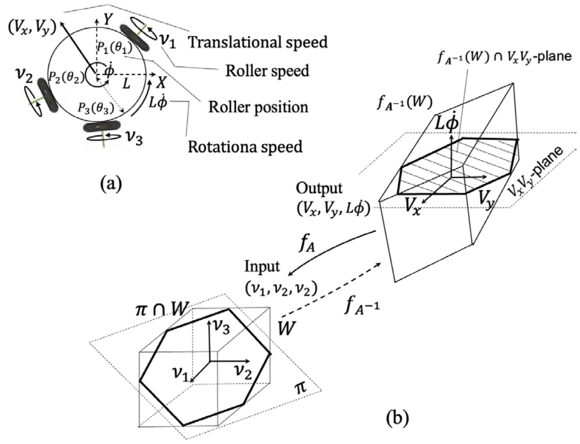

Fig. 2 Correspondence omni-roller speed $[v_1, v_2, v_3]^{\boldsymbol{T}}$ and robot speed elements $[V_x, V_y, \dot{\phi}L]^{\boldsymbol{T}}$: (a). mobile robot and (b). transformation mapping.

$$f_{A^{-1}}(W) \cap \{V_x V_y - \text{plane}\}$$
$$= \{(V_x, V_y, 0) |\, |v_1|, |v_2|, |v_3| \leq 1\} \quad (1)$$

Where

$$f_{A^{-1}}(W) = \{(V_x, V_y, L\dot{\phi}) |\, |v_1|, |v_2|, |v_3| \leq 1\} \quad (2)$$

$$= \{(v_1, v_2, v_3) | |v_1|, |v_2|, |v_3| \leq 1\} \quad (3)$$

Inverse kinematics (f_A : $[V_x, V_y, \dot{\phi}L]^{\boldsymbol{T}} \to [v_1, v_2, v_3]^{\boldsymbol{T}}$) is represented as the following Eq. (4).

$$\begin{bmatrix} v_1 \\ v_2 \\ v_3 \end{bmatrix} = \begin{bmatrix} -\sin\theta_1 & \cos\theta_1 & 1 \\ -\sin\theta_2 & \cos\theta_2 & 1 \\ -\sin\theta_3 & \cos\theta_3 & 1 \end{bmatrix} \begin{bmatrix} V_x \\ V_y \\ L\dot{\phi} \end{bmatrix} \quad (4)$$

Additionally, forward kinematics ($f_{A^{-1}}$: $[v_1, v_2, v_3]^{\boldsymbol{T}} \to [V_x, V_y, \dot{\phi}L]^{\boldsymbol{T}}$) is represented using Eq. (5).

$$\begin{bmatrix} V_x \\ V_y \\ L\dot{\phi} \end{bmatrix} = \frac{1}{\det\boldsymbol{A}} \begin{bmatrix} -\sin\theta_1 & \cos\theta_1 & 1 \\ -\sin\theta_2 & \cos\theta_2 & 1 \\ -\sin\theta_3 & \cos\theta_3 & 1 \end{bmatrix}^{-1} \begin{bmatrix} v_1 \\ v_2 \\ v_3 \end{bmatrix} \quad (5)$$

3. Analysis for sectional shape and area

As a special case, a sectional area is analyzed in the case of isosceles triangle-like–three-roller arrangement in [11]. Meanwhile, in this study, a more general case is analyzed regarding sectional shapes.

3.1. *Setup for domain and division*

Cubic domain W is composed following 8-apexes $\boldsymbol{P} = (1, 1, 1)$, $\boldsymbol{Q} = (-1, 1, 1)$, $\boldsymbol{R} = (-1, -1, 1)$, $\boldsymbol{S} = (1, -1, 1)$, $\acute{\boldsymbol{P}} = (1, 1, -1)$, $\acute{\boldsymbol{Q}} = (-1, 1, -1)$, $\acute{\boldsymbol{R}} = (-1, -1, -1)$, $\acute{\boldsymbol{S}} = (1, -1, -1)$.

Focusing on $L\dot{\phi}$-component of Eq. (5), we define $\theta_3 = 0°$.

$$F(v_1, v_2, v_3) = \begin{bmatrix} v_1 \\ v_2 \\ v_3 \end{bmatrix} \cdot \begin{bmatrix} n_1 \\ n_2 \\ n_3 \end{bmatrix} \tag{6}$$

Where

$$n_1 = -\sin\theta_2 \tag{7}$$

$$n_2 = \sin\theta_1 \tag{8}$$

$$n_3 = -\sin(\theta_1 - \theta_2) \tag{9}$$

In the case of translational motion, $\dot{\phi} = 0$ is equivalent to $F(v_1, v_2, v_3) = 0$, which is a linear equation with respect to $v_1, v_2,$ and v_3. Therefore, geometrically, it can be represented as a plane with an origin and normal vector $\boldsymbol{n} = [n_1, n_2, n_3]^{\boldsymbol{T}}$. Thus, the arrangement position of roller is completely dependent on $\boldsymbol{n}$.

As shown in Fig. 3, $D = \{(v_1, v_2)|\ |v_1|, |v_2| \leq 1\}$ is a sectional domain of W by $v_3 = 0$ and can be decomposed to the following four parts: D_{++}, D_{-+}, D_{--}, and D_{+-}.

$$D_{++} = \{(v_1, v_2)|\ 0 < v_1 \leq 1, 0 < v_2 \leq 1\} \tag{10}$$

$$D_{-+} = \{(v_1, v_2)|\ -1 < v_1 \leq 0, 0 < v_2 \leq 1\} \tag{11}$$

$$D_{--} = \{(v_1, v_2)| -1 < v_1 \leq 0, -1 < v_2 \leq 0\} \tag{12}$$

$$D_{+-} = \{(v_1, v_2)|\ 0 < v_1 \leq 1, -1 < v_2 \leq 0\} \tag{13}$$

In this study, we focus on domain D_{++}(grey highlight in Fig. 3). It can be decomposed into two parts by a sign of n_3. From $0° < \theta_1, \theta_2 < 360°$, and $\theta_1 \neq \theta_2$, (θ_1, θ_2) is satisfied with following inequality.

$$-360° < \theta_1 - \theta_2 < 360°, \theta_1 \neq \theta_2 \tag{14}$$

In the case of $n_3 > 0$, it is equivalent to $180° < \theta_1 - \theta_2 < 360°$ and $-180° < \theta_1 - \theta_2 < 0°$ ($-360° + \theta_1 < \theta_2 < -180° + \theta_1$). Thus, the following inequality is obtained.

$$\theta_1 < \theta_2 < 180° + \theta_1 \tag{15}$$

In the case of $n_3 < 0$, it is equivalent to $0° < \theta_1 - \theta_2 < 360°$ and $-360° < \theta_1 - \theta_2 < -180°$ ($-180° + \theta_1 < \theta_2 < \theta_1$). Thus, the following inequality is given.

$$180° + \theta_1 < \theta_2 < 360° + \theta_1 \tag{16}$$

Using Eq. (15) and Eq. (16), D_{++} can be decomposed to domains D^-_{++} and D^+_{++}.

$$D^-_{++} = \{(\theta_1, \theta_2)|\ \theta_1 < \theta_2 \leq 360°, 0° < \theta_1 \leq 180°\} \tag{17}$$

$$D^+_{++} = \{(\theta_1, \theta_2)|\ 180° < \theta_2 \leq \theta_1, 0° < \theta_1 \leq 180°\} \tag{18}$$

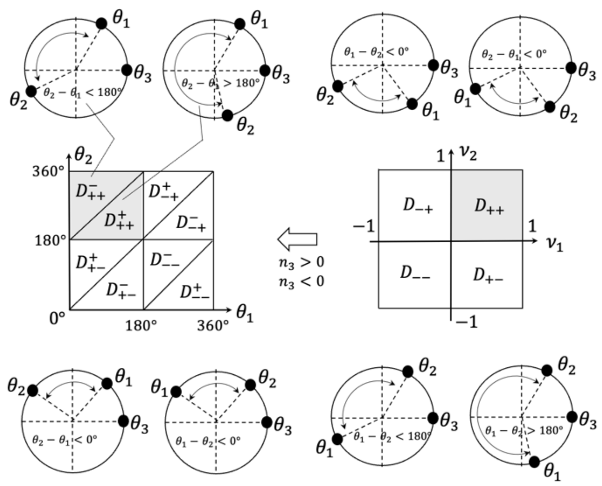

Fig. 3 Three-roller arrangement poteen corresponding to domain D^-_{++} and D^+_{++}.

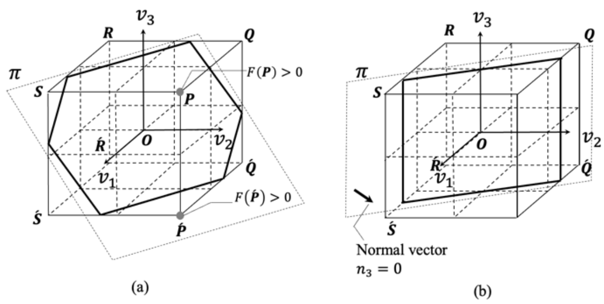

Fig. 4 Classification of the sectional shape of a cube in the case of domain D^-_{++}: (a). hexagon and (b). rhombus shapes.

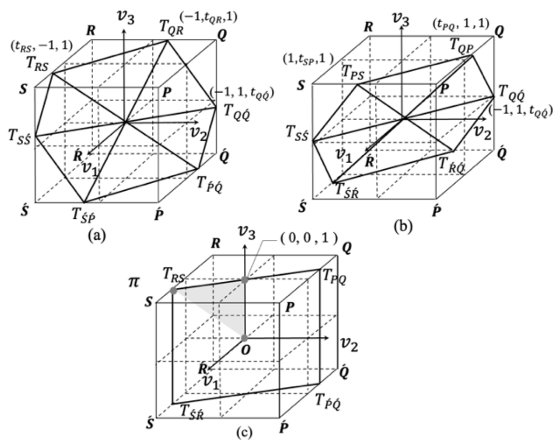

Fig. 5 Classification of sectional in D_{++} (a). The case of hexagon domain D^-_{++} (b), hexagon domain D^+_{++} (c), and rhombus domain D_{++}

3.2. *Analysis of sectional shapes*

The sectional shape condition in D_{++}^{-} is considered. From Eq. (17), (θ_1, θ_2) is satisfied because $0° < \theta_1 \leq 180°$ and $180° < \theta_2 \leq 360°$.

In cases where $n_3 \neq 0$ and $\theta_2 - \theta_1 < 180°$, $F(1,1,1)$ and $F(1,1,-1)$ are calculated as follows:

$$F(1,1,1) = \sin\theta_1 - \sin\theta_2 - \sin(\theta_1 - \theta_2) > 0 \tag{19}$$

$$F(1,1,-1) = \sin\theta_1 - \sin\theta_2 + \sin(\theta_1 - \theta_2) \tag{20}$$

$$= \sin\theta_1 + \sin(-\theta_2) + \sin(\theta_1 + (-\theta_2)) \tag{21}$$

$$= \sin\theta_1 + \sin(-\theta_2) + \sin\theta_1 \cos(-\theta_2) + \cos\theta_1 \sin(-\theta_2) \tag{22}$$

From $1 + \cos(-\theta_2) > 0$ and $1 + \cos\theta_1 > 0$,

$$= \sin\theta_1 (1 + \cos(-\theta_2)) + \sin(-\theta_2)(1 + \cos\theta_1) > 0 \tag{23}$$

Thus, $\boldsymbol{P}(1,1,1)$ and $\boldsymbol{\acute{P}}(1,1,-1)$ are up word on of plane's normal vector direction. Thus, the sectional shape of the domain is hexagon (Fig. 4(a)).

In the case where $n_3 = 0$, $\boldsymbol{n}$ is parallel to $\{V_x V_y - \text{plane}\}$. Thus, the sectional shape of the domain is rhombus (Fig. 4(b)).

$\pi \cap W$ is satisfied as the following property.

Property1

The sectional shape has a line symmetry with respect to the origin and can be divided into the following two classes:

$|\theta_1 - \theta_2| \neq 180° \Longrightarrow$ Hexagon

$|\theta_1 - \theta_2| = 180° \Longrightarrow$ Rhombus

3.3. *Derivation of sectional area function*

$\pi \cap W =$ Hexagon $\boldsymbol{T_{RS}T_{S\acute{S}}T_{\acute{P}\acute{S}}T_{\acute{P}\acute{Q}}T_{Q\acute{Q}}T_{QR}}$ is decomposed to the following six parts: $\triangle\, \boldsymbol{O\, T_{RS}T_{QR}}$, $\triangle\, \boldsymbol{O\, T_{QR}T_{Q\acute{Q}}}$, $\triangle\, \boldsymbol{O\, T_{Q\acute{Q}}T_{RS}}$, $\triangle\, \boldsymbol{O\, T_{\acute{P}\acute{S}}T_{\acute{P}\acute{Q}}}$, $\triangle\, \boldsymbol{O\, T_{\acute{P}\acute{S}}T_{S\acute{S}}}$, and $\triangle\, \boldsymbol{O\, T_{Q\acute{Q}}T_{\acute{P}\acute{Q}}}$. Furthermore, the transformation mapping of $f_{A^{-1}}$ shows that $f_{A^{-1}}(\boldsymbol{O}) = \boldsymbol{O}$ and $f_{A^{-1}}(\pi \cap W)$ is represented as sum of $\triangle\, \boldsymbol{O}\, f_{A^{-1}}(\boldsymbol{T_{RS}}) f_{A^{-1}}(\boldsymbol{T_{QR}})$, $\triangle\, \boldsymbol{O}\, f_{A^{-1}}(\boldsymbol{T_{QR}}) f_{A^{-1}}(\boldsymbol{T_{Q\acute{Q}}})$, $\triangle\, \boldsymbol{O}\, f_{A^{-1}}(\boldsymbol{T_{Q\acute{Q}}}) f_{A^{-1}}(\boldsymbol{T_{RS}})$, $\triangle\, \boldsymbol{O}\, f_{A^{-1}}(\boldsymbol{T_{\acute{P}\acute{S}}}) f_{A^{-1}}(\boldsymbol{T_{\acute{P}\acute{Q}}})$, $\triangle\, \boldsymbol{O}\, f_{A^{-1}}(\boldsymbol{T_{\acute{P}\acute{S}}}) f_{A^{-1}}(\boldsymbol{T_{S\acute{S}}})$, and $\triangle\, \boldsymbol{O}\, f_{A^{-1}}(\boldsymbol{T_{Q\acute{Q}}}) f_{A^{-1}}(\boldsymbol{T_{\acute{P}\acute{Q}}})$.

Area of $f_{A^{-1}}(\pi \cap W)$ is defined as $D_{Sec}(\theta_1, \theta_2)$ ($(\theta_1, \theta_2) \in D_{++}$). It is decomposed into the following $D_{Sec}^{+}(\theta_1, \theta_2)$ ($(\theta_1, \theta_2) \in D_{++}^{+}$) and $D_{Sec}^{-}(\theta_1, \theta_2)$ ($(\theta_1, \theta_2) \in D_{++}^{-}$), which are function depended on roller contact position $(\theta_1, \theta_2, 0°)$.

The opposite sides are parallel and have the same length. Thus, hexagon $f_{A^{-1}}(\pi \cap W)$ has a symmetry with respect to origin $\boldsymbol{O}$. Thus, in the case of hexagon, $D_{Sec}^{+}(\theta_1, \theta_2)$ and $D_{Sec}^{-}(\theta_1, \theta_2)$ are derived as the sum of three triangle areas (Fig. 5(a)(b)). Furthermore, in the case of rhombus, $D_{Sec}(\theta_1, \theta_2)$ is derived as the sum of the same eight triangle areas (Fig. 5(c)).

$$\begin{aligned} D_{Sec}^{+}(\theta_1, \theta_2) = & \left\| f_{A^{-1}}(\boldsymbol{T_{RS}}) \times f_{A^{-1}}(\boldsymbol{T_{QR}}) \right\| \\ & + \left\| f_{A^{-1}}(\boldsymbol{T_{QR}}) \times f_{A^{-1}}(\boldsymbol{T_{Q\acute{Q}}}) \right\| \\ & + \left\| f_{A^{-1}}(\boldsymbol{T_{S\acute{S}}}) \times -f_{A^{-1}}(-\boldsymbol{T_{RS}}) \right\| \\ & (\, |\theta_1 - \theta_2| \neq 180°, (\theta_1, \theta_2) \in D_{++}^{+} \,) \end{aligned} \tag{24}$$

$$\begin{aligned} D_{Sec}^{-}(\theta_1, \theta_2) = & \left\| f_{A^{-1}}(\boldsymbol{T_{PS}}) \times f_{A^{-1}}(\boldsymbol{T_{QP}}) \right\| \\ & + \left\| f_{A^{-1}}(\boldsymbol{T_{QP}}) b \times f_{A^{-1}}(\boldsymbol{T_{Q\acute{Q}}}) \right\| \\ & + \left\| f_{A^{-1}}(\boldsymbol{T_{S\acute{S}}}) \times -f_{A^{-1}}(-\boldsymbol{T_{PS}}) \right\| \\ & (\, |\theta_1 - \theta_2| \neq 180°, (\theta_1, \theta_2) \in D_{++}^{-} \,) \end{aligned} \tag{25}$$

$$\begin{aligned} D_{Sec}(\theta_1, \theta_2) = & \, 4 \left\| f_{A^{-1}}(\boldsymbol{T_{RS}}) \times f_{A^{-1}}(0,\ 0,\ 1) \right\| \\ & (\, |\theta_1 - \theta_2| = 180°, (\theta_1, \theta_2) \in D_{++} \,) \end{aligned} \tag{26}$$

Where $\boldsymbol{T_{RS}}(t_{RS}, -1, 1)$, $\boldsymbol{T_{QR}}(-1, t_{QR}, 1)$, $\boldsymbol{T_{SP}}(1, t_{SP}, 1)$, $\boldsymbol{T_{PQ}}(t_{PQ}, 1, 1)$, and $\boldsymbol{T_{Q\acute{Q}}}(-1, 1, t_{Q\acute{Q}})$.

$$t_{RS} = \frac{-\sin\theta_1 - \sin(\theta_1 - \theta_2)}{\sin\theta_2} \tag{27}$$

$$t_{QR} = \frac{-\sin\theta_2 + \sin(\theta_1 - \theta_2)}{\sin\theta_1} \tag{28}$$

$$t_{SP} = \frac{\sin\theta_2 + \sin(\theta_1 - \theta_2)}{\sin\theta_1} \tag{29}$$

$$t_{PQ} = \frac{\sin\theta_1 - \sin(\theta_1 - \theta_2)}{\sin\theta_2} \tag{30}$$

$$t_{Q\acute{Q}} = \frac{\sin\theta_1 + \sin\theta_2}{\sin(\theta_1 - \theta_2)} \tag{31}$$

4. Simulation

This section presents the simulation findings, including the horizontal cross-sectional area D_{Sec}, as evaluation values.

Section 4.1 shows the case of a roller arrangement that has a line symmetry with respect to the x-axis.

Section 4.2 shows the case of a roller arrangement that has a point symmetry with respect to the origin.

Simulations were performed on three various roller arrangement patterns. Types (A)-(E) are arranged in the shape of a triangle, corresponding to Fig. 1(a)-(e), respectively.

4.1. Case of line-symmetry arrangement with respect to the x-axis

Fig. 6 (b)(a)(c) shows the shape in the case of a triangle that has a line symmetry with respect to the x-axis.

$D^{+}_{Sec}(\theta, 2\pi - \theta)$ (substituting Eq. (24) to $\theta_1 = \theta$ and $\theta_2 = 2\pi - \theta$ for $90° \leq \theta < 180°$) and $D^{-}_{Sec}(\theta, 2\pi - \theta)$ (substituting Eq. (25) to $\theta_1 = \theta$ and $\theta_2 = 2\pi - \theta$ for $0° \leq \theta < 90°$) are analyzed. They are set up as θ_i ($i = 1,2,3$) as follows:

Type(B):$(\theta_1, \theta_2, \theta_3) = (60°, 300°, 0°)$

Type(A):$(\theta_1, \theta_2, \theta_3) = (90°, 270°, 0°)$

Type(C): $(\theta_1, \theta_2, \theta_3) = (120°, 240°, 0°)$ and $L = 1$[m].

Fig. 6(d)(a)(e) show an outline of the velocity distributions for Type(A), Type(B), and Type(C). Their shapes are hexagon, square, and hexagon, respectively.

Fig. 7 shows the shape in the case of a triangle that has a point symmetry with respect to origin $\boldsymbol{O}$. $D_{Sec}(\theta, 2\pi - \theta)$ (substituting Eq. (26) to $\theta_1 = \theta$ and $\theta_2 = 2\pi - \theta$ for $90° \leq \theta < 180°$), as a result, $D_{Sec}(90°) = 4.05[m/s]^2$ and it takes minimal value $D_{Sec}(60°)$ and $D_{Sec}(120°) = 3.85\ [m/s]^2$. Moreover, $D_{Sec}(0°) = \infty$ and $D_{Sec}(180°) = \infty$.

The result shows that Type(B) and Type(C) are the rollers arrangement with poorest efficiency for only translational motion.

4.2. Case of point-symmetry arrangement with respect to origin

Fig. 6(d)(a)(e) shows the shape in the case of a triangle that has a point symmetry with respect to origin $\boldsymbol{O}$.

$D_{Sec}(\theta, 2\pi - \theta)$ (substituting Eq. (26) to $\theta_1 = \theta$ and $\theta_2 = 2\pi + \theta$ for $0° \leq \theta < 180°$) is analyzed and is set up as θ_i ($i = 1,2,3$) as follows:

Type(D): $(\theta_1, \theta_2, \theta_3) = (60°, 240°, 0°)$

Type(A): $(\theta_1, \theta_2, \theta_3) = (90°, 270°, 0°)$

Type(E): $(\theta_1, \theta_2, \theta_3) = (120°, 300°, 0°)$

Fig. 6 shows an outline of velocity distributions for Type(D), Type(A), and Type(E), represented as hexagon, square, and hexagon, respectively.

As shown in Fig. 8, it is symmetry function and takes minimal value $D_{Sec}(90°) = 4.05[m/s]^2$. In addition, $D_{Sec}(0°)$ and $D_{Sec}(180°) = \infty$.

The result shows that Type(A) is the smallest and efficient when only translational motion is assumed.

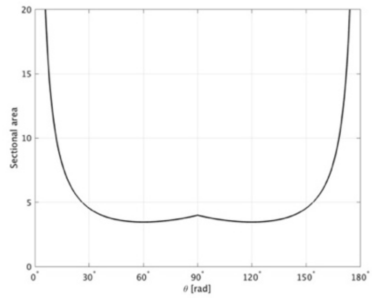

Fig. 7 Behaviors of $D^{-}_{Sec}(\theta, 2\pi - \theta)$ $(0° \leq \theta < 180°)$ and $D^{+}_{Sec}(\theta, 2\pi - \theta)(90° \leq \theta < 180°)$.

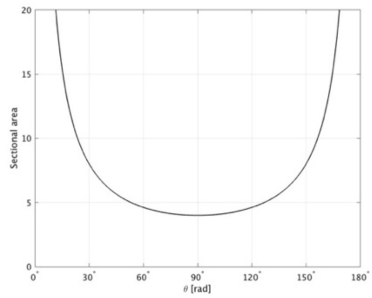

Fig. 8 Behaviors of $D_{Sec}(\theta, 2\pi - \theta)(0° \leq \theta < 180°)$

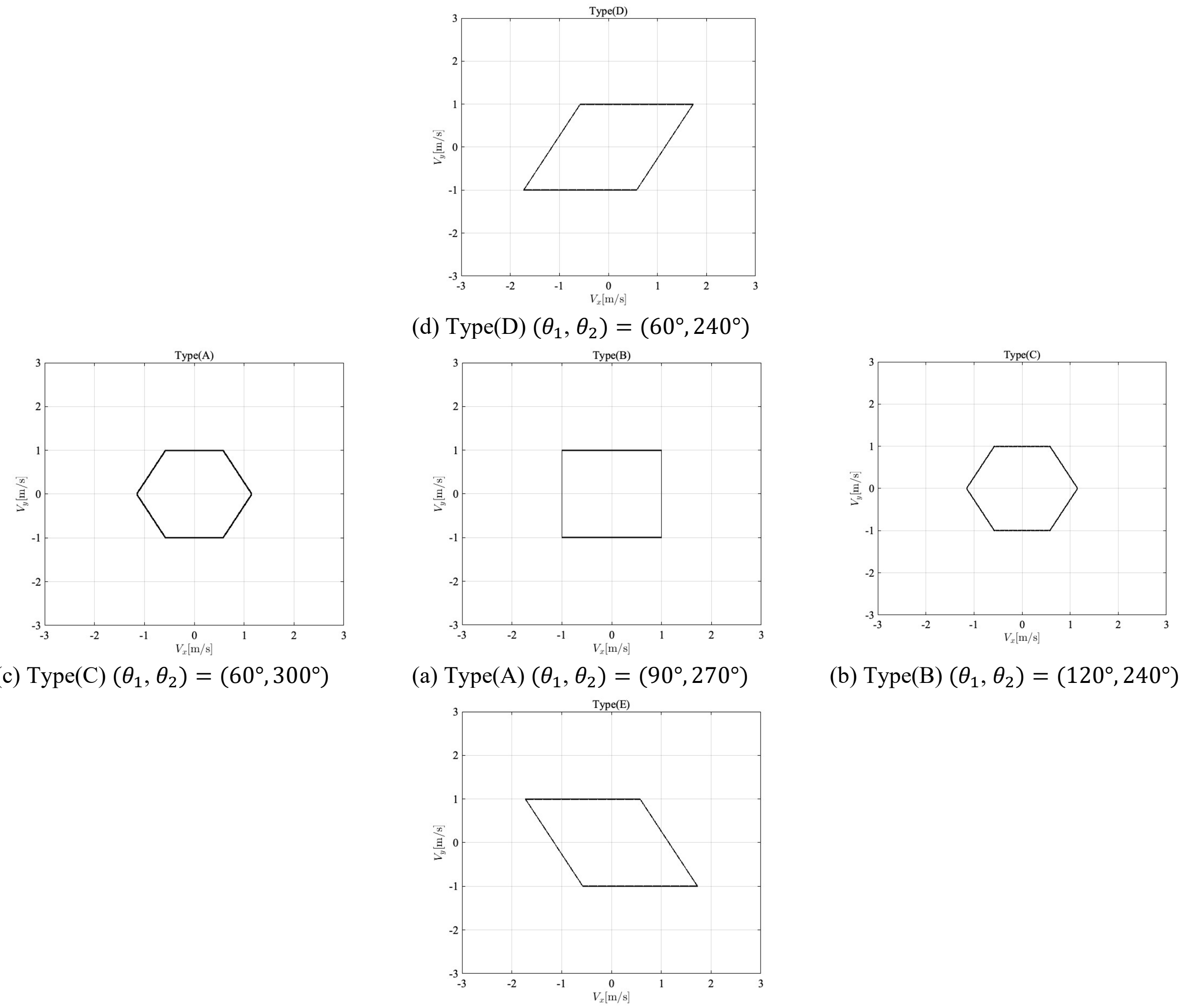

(d) Type(D) $(\theta_1, \theta_2) = (60°, 240°)$

(c) Type(C) $(\theta_1, \theta_2) = (60°, 300°)$ (a) Type(A) $(\theta_1, \theta_2) = (90°, 270°)$ (b) Type(B) $(\theta_1, \theta_2) = (120°, 240°)$

(e) Type(E) $(\theta_1, \theta_2) = (120°, 300°)$

Fig. 6 Simulation result for the roller arrangement in the case of symmetry (a)(b)(c), line symmetry. (a)(d)(e), and point symmetry

5. Conclusion

In this study, a function was successfully derived to evaluate the efficiency of only the translational movement in a mobile mechanism equipped with three omni-rollers. Furthermore, the distribution of the translational velocity of the robot was analyzed through simulation, and the roller arrangement with the poorest efficiency was clarified.

The future works will focus on the efficiency of movement when the roller direction is changed arbitrarily in mobile robots.

Acknowledgment

This work was supported by JSPS Grant-in-Aid for Scientific Research 23 K13279.

References

1. J. Tang, K. Watanabe, et al., "Autonomous Control for an Omnidirectional Mobile Robot with the Orthogonal-Wheel Assembly," Journal of the Robotics Society of Japan. Vol. 17, No. 1, pp. 51-60, 1999.
2. Y. Yasohara, K. Shimizu, et al., Development of Ball Handling Mechanism for RoboCup MSL, *30th Fussy System Symposium*, pp. 616-617, 2014.
3. S. Chikushi, M. Kuwada, et al., Development of Next-Generation Soccer Robot "Musashi150" for RoboCup MSL, *30th Fussy System Symposium*, pp. 624-627, 2014.
4. R. Junkai, X. Chenggang, X. Junhao, et al., A Control System for Active Ball Handling in the RoboCup Middle Size League, *Chinese Control and Decision Conference (CCDC) 2016.*
5. K. Kimura, K. Ogata, K. Ishii, Novel Mathematical Modeling and Motion Analysis of a Sphere

Considering Slipping, Journal of Robotics, Networking and Artificial Life, Vol. 6, No. 1, pp. 27-32, 2019.
6. K. Kimura, K. Ogata, H. Hirai, T. Ueda, K. Ishii, Forward Kinematic of a Sphere Considering Slipping and Motion Analysis in Three Rollers, Journal of Advances in Artificial Life Robotics Vol. 10, No. 1, 2023.
7. K. Kimura, K. Ishii, The Spherical Robot Transfer Problem With Minimal Total Kinetic Energy, *Proceedings of International Conference on Artificial ALife and Robotics (ICAROB2021)*, pp.266-270, 2021.
8. K. Kimura, K. Ishii, Efficiency Problem of Spherical Robot in Transfer Kinetic Energy, Journal of Robotics, Networking and Artificial Life, Vol. 9, No. 1, pp. 87-92, 2022.
9. K. Kimura, Y. Abematsu, H. Hirai, K. Ishii, Evaluation of Two Roller Arrangement on a Hemisphere by Kinetic Energy, Journal of Robotics, Networking and Artificial Life, Vol. 9, No. 3, pp. 233-239, 2022.
10. K. Kimura, Y. Shigyo, K. Ishii, An Analysis of Robot Speed Efficiency for Mobile Robot Adapted Three Omni Rollers Using Linear Transformation, Journal of Advances in Artificial Life Robotics Vol. 3, No. 4, pp. 242-249, 2023.
11. K. Kimura, K. Ishii, An Analysis of Translational Motion for a Mobil Robot with Line-Symmetric Rollers Arrangement, *Proceedings of International Conference on Artificial ALife and Robotics (ICAROB2024),* pp.603-606, 2024.

Authors Introduction

Dr. Kenji Kimura

He is a Lecturer at the Department of Control Engineering, National Institute of Technology, Matsue College, and a Visiting Associate Professor at Chuo University. He received his ME (mathematics) from Kyushu University in 2002 and his PhD (engineering) from the Kyushu Institute of Technology in 2020. His research interests are spherical mobile robots.

Dr. Kazuo Ishii

He is a Professor in the Kyushu Institute of Technology, where he has been since 1996. He received his Ph.D. degree in engineering from University of Tokyo, in 1996. His research interests span both ship marine engineering and Intelligent Mechanics. He holds five patents derived from his research.